

# Inverse anisotropic catalysis and complexity

Mojtaba Shahbazi \*

Tabiat Modares University, Tehran, Iran

January 2, 2024

## Abstract

In this work the effect of anisotropy on computational complexity is considered by CA proposal in holographic two-sided black brane dual of a strongly coupled gauge theory. It is shown that due to confinement-deconfinement phase transition there are two different behaviors: by increase in anisotropy there would be an increase in complexity growth rate in small anisotropy and a decreases in the complexity growth rate in large anisotropy. In the extreme case the very large anisotropy leads to the unity of the complexity growth rate and complexity itself, it means that in this case getting the target state from the reference state is reachable by no effort. Moreover, we suggest that  $\frac{1}{M} \frac{dC}{dt}$  is a better representation of system degrees of freedom rather than the complexity growth rate  $\frac{dC}{dt}$  and show that how it is related to inverse anisotropic catalysis. In addition, we consider the one-sided black brane dual to the quantum quench and showed that increase in anisotropy comes with decrease in complexity regardless of the anisotropy value which is due to the fact that the system do not experience a phase transition.

*Dedicated to Iranian women especially my mom that has just passed away.*

## 1 Introduction

Gauge/gravity duality provides us a very handy technique to study strongly interacting quantum field theories; moreover, it brings us a geometric description of quantum systems [1]. In this framework the theory of gravitation lives in the bulk and the quantum theory on the boundary. By a dictionary quantities in the bulk are correspondent to quantities on the boundary. The notion of computational complexity has been introduced [2] to further study of interior of black holes. Computational complexity is a notion in computer science that comes into quantum information as a minimum number of required quantum gates to make a target state out of a reference state. There are some proposals for its holographic dual of the notion such as complexity equals volume [3], known as CV proposal that relates volume of Einstein-Rosen bridges (ERB), a geometric notion to computational complexity in quantum side. The other proposal relates complexity to action [4], known as CA proposal that corresponds action of a gravitational theory in Wheeler-DeWitt patch (WDW) to computational complexity and a proposal CV-2.0 relates complexity to spacetime volume restricted to WDW patch [5]. Recently, it has been proposed an infinite class of surfaces as a holographic candidate of complexity [6].

It is found that there is an upper limit for the rate of complexity change which is called Lloyd limit [7]:

$$\frac{dC}{dt} \leq \frac{2M}{\pi}, \quad (1)$$

---

\*mojtaba.shahbazi@modares.ac.ir

where  $M$  is mass of the black hole. Lloyd limit is violated in several theories [8–12]. There are some modifications that can preserve Lloyd limit in some theories; however, left the others violated [13–15].

Anisotropic strongly coupled systems appear in various condensed matter systems in the presence of an external field such as electric or magnetic field, or in the initial stages of quark-gluon plasma in which produced in non-central heavy ion collisions. Strongly coupled anisotropic QFTs have been studied holographically in various gravity models such as: electric/magnetic sources [16–23] and dilatonic/axionic sources [24–28]. It has been shown that a non-conformal and anisotropic system with strong interaction is correspondent to an Einstein-Dilaton-Axion gravity in which the dilaton field  $\phi$  is dual to  $TrF^2$  in gauge theory and the axion field  $\xi$  to  $TrF \wedge F$  [28]. Furthermore, in [28] it is shown that confinement-deconfinement transition temperature decreases by anisotropy that is similar to lattice QCD result known as inverse magnetic catalysis (IMC), in which an external magnetic field leads to the change of the critical temperature for the chiral condensation where the magnetic field causes the anisotropy in the same manner of [28]. However, the gravity model in [28] describes an uncharged plasma and the lattice QCD a charged one, then it appears that IMC-like effect could occur in uncharged plasmas in other words, the origin of IMC is not the magnetic field but the anisotropy [28] and the idea is confirmed in [23] where there is anisotropy and no magnetic field and coined the phenomenon as inverse anisotropic catalysis (IAC). Nonetheless, IMC does not appear in perturbative QCD but the magnetic catalysis (MC). There are models showing the both IMC and MC for different values of the magnetic field [29] and considering effect of different angles of magnetic field and the anisotropy arises due to the different pressure gradient in plasma on the system [30].

In this paper, we are going to consider an Einstein-Dilaton-Axion theory to find how anisotropy affects complexity via CA proposal for a two-sided black brane with Lifshitz anisotropic hyper-scaling violating exponent. This model has been considered in holography [31–34]. In addition, we consider the Vaidya metric which is dual to a global quantum quench in dual field theory in order to study how closed quantum systems approach to their equilibrium. It is revealed that complexity growth rate decreases when the anisotropy increases because the anisotropy could be caused by a magnetic field as in [16–23]; in addition, the more decrease in complexity, the less effort we pay, in other words the distance between states (reference and target states) in complexity space decreases; moreover, in asymptotic behavior when complexity goes to unity at large anisotropy parameter, it seems that in the system there is no difficulty to reach the target state from the reference state, then target and reference seem to be coincided. The decrease in the complexity growth rate could be addressed to the dilaton field which is in charge of open strings coupling in string theory. It means that the more anisotropy, the more coupling and as a result the less complexity rate. The same calculation in an anisotropic black brane has been conducted for a perturbative solution in terms of anisotropy parameter [42] and expecting the Lloyd bound violation in large anisotropy parameter due to the presence of conformal anomaly; however, the model we consider here is a non-perturbative solution, it means that we can study the effect of anisotropy on complexity all the way from small anisotropy parameter to large one and as will be shown there are two different behaviors of anisotropy on complexity which stems from the confinement-deconfinement phase transition as reported in [28]. Although, the Lloyd bound is respected in small anisotropy, it violates in the large anisotropy. However, in one-sided black brane the Lloyd bound is independent of the effect of anisotropy.

By the way, the complexity growth rate has been considered as representing system degrees of freedom [47]. Nonetheless, we show that the complexity growth rate itself is not a proper representation of the system degrees of freedom, but  $\frac{1}{M} \frac{dC}{dt}$ <sup>1</sup> does and show that how it is related to IAC.

The rest of the paper is organized as follows: in section 2, complexity of Einstein-Dilaton-

---

<sup>1</sup>For a closed system  $M$  is constant. It seems that when the mass is changed, the Hilbert space of the system is changed. However, we can consider them as a perturbation and compare the two Hilbert spaces.

Axion gravity for two-sided black brane is computed and the Lloyd bound is considered. In section 3 the case of one-sided black brane is calculated where the same result appears. In addition, the relation between complexity, degrees of freedom and IAC is discussed in 4. At the end it comes to a conclusion in 5.

## 2 Complexity of two-sided black brane

In this section on shell action in WDW patch is considered for black branes with hyperscaling violating exponent. The gravitational theory could be given by the following action:

$$S = \frac{1}{16\pi G} \int d^{d+2}x \sqrt{-g} \left( R - \frac{1}{2}(\partial\phi)^2 + V(\phi) - \frac{1}{2}Z(\phi)(\partial\xi)^2 \right), \quad (2)$$

where  $Z$  is coupling of dilaton field  $\phi$  to axion field  $\xi$  and for strongly-coupled gauge theories the coupling and dilaton potential would be [28]:

$$V(\phi) = 6e^{\tau\phi}, \quad Z(\phi) = e^{2\beta\phi}. \quad (3)$$

A good realization of 5D Einstein-Dilaton-Axion theory can be found in terms of D3/D7 branes in IIB string theory by  $Z(\phi) = e^{2\phi}$  and  $V(\phi) = 12$  [35]. The solution of the action (2) is a Lifshitz anisotropic hyperscaling violation metric which comprises an arbitrary critical exponent  $z$  and a hyperscaling violation exponent  $\theta$  expressed in terms of constants  $\alpha$  and  $\beta$ . The metric of the dual geometry would be:

$$ds^2 = \omega r^{\frac{2\theta}{dz}} \left( \frac{-f dt^2}{r^2} + \frac{dr^2}{r^2 f} + \frac{d\vec{x}^2}{r^2} + \frac{dy^2}{\kappa r^{\frac{2}{z}}} \right), \quad (4)$$

and the function  $f$  is given:

$$f = 1 - \left( \frac{r}{r_h} \right)^{d + \left( \frac{1-\theta}{z} \right)}, \quad (5)$$

where  $r_h$  is the horizon radius and the thermodynamical quantities are as follows:

$$T = \frac{d + \frac{1-\theta}{z}}{4\pi r_h}, \quad (6)$$

$$M = \frac{V}{16\pi G} \sqrt{\frac{\omega^d}{\kappa}} \frac{dz + 1 - z - \theta}{z} \frac{1}{r_h^{d + \frac{1-\theta}{z}}}. \quad (7)$$

By null energy condition we have:

$$(z-1)(1+dz-\theta) \geq 0, \quad \theta^2 + dz(1-\theta) - d \geq 0. \quad (8)$$

One can find eligible ranges for  $z$  and  $\theta$ , that is revealed  $z_- \geq z, z \geq z_+$  and  $\theta_- \geq \theta, \theta \geq \theta_+$ :

$$\theta_{\pm} = \frac{1}{2} \left( dz \pm \sqrt{(dz)^2 - 4dz + 4d} \right), \quad z_{\pm} = \frac{1}{2d} \left( d + \theta - 1 \pm |d - \theta + 1| \right). \quad (9)$$

In the following we suppose that  $d > z$  and  $d > \theta$  such that satisfy null energy condition (NEC).

The trace of the equation of motion leads to:

$$R - \frac{1}{2}(\partial\phi)^2 - \frac{1}{2}e^{2\beta\phi}(\partial\xi)^2 + \left( \frac{d+2}{d} \right) 6e^{\tau\phi} = 0, \quad (10)$$

then the density of the Lagrangian reads as:

$$\sqrt{-g} \left( R - \frac{1}{2}(\partial\phi)^2 - \frac{1}{2}e^{2\beta\phi}(\partial\xi)^2 + 6e^{\tau\phi} \right) = - \left( \sqrt{\frac{\omega^{d+2}}{\kappa}} r^{\frac{(d+2)\theta}{dz} - \frac{1}{z} - (d+1)} \right) \frac{12}{d} e^{\tau\phi}. \quad (11)$$

For the IR limit one can find exact solution [28]:

$$\phi = c_1 \log(c_2 r) + c_3, \quad (12)$$

where  $c_2 = \omega^{\frac{dz}{2\theta-2dz}}$  that can be called anisotropic parameter,  $\kappa = \frac{1}{a} c_2^{\frac{2d-2dz}{dz}}$  and  $a, c_1, c_3$  are constant. The right hand side of eq. (11) would be:

$$-\frac{12}{d} \sqrt{\frac{\omega^{d+2}}{\kappa}} e^{\tau c_3} c_2^{\tau c_1} r^{\frac{(d+2)\theta}{dz} - \frac{1}{2} - (d+1) + \tau c_1}, \quad (13)$$

then eq. (2) leads to:

$$S = -\frac{3V_d}{4\pi G d} \sqrt{\frac{\omega^{d+2}}{\kappa}} e^{\tau c_3} c_2^{\tau c_1} \int dt dr r^{\frac{(d+2)\theta}{dz} - \frac{1}{2} - (d+1) + \tau c_1}. \quad (14)$$

If one is interested in computing the action in WDW patch should add some terms to the action [36, 37]:

$$S = \frac{1}{16\pi G} \int d^{d+2}x \sqrt{-g} \left( R - \frac{1}{2} (\partial\phi)^2 + V(\phi) - \frac{1}{2} Z(\phi) (\partial\xi)^2 \right) + \frac{1}{8\pi G} \int d^{d+1}x \sqrt{-h} K \pm \frac{1}{8\pi G} \int d^d x \sqrt{-\gamma} \log(a_{ij}), \quad (15)$$

where for two light-like vectors and for a light-like and a time-like vector respectively there would be:

$$a_{ij} = \left| \frac{n_i \cdot n_j}{2} \right|, \quad a_{ij} = |n_i \cdot k_j|. \quad (16)$$

Gibbons-Howking-York(GHY) term is read as follows:

$$S_{\text{GHY}} = \frac{\text{sgn}(j)}{8\pi G} \int_{\Sigma} \sqrt{-h} K d^{d+1}x, \quad (17)$$

$\text{sgn}(j)$  for time-like surface  $\Sigma$  is 1 and for space-like surface if it lies to the past of the bulk is 1 otherwise -1 and for light-like surfaces GHY term vanishes.  $K$  is extrinsic curvature of the (d+1)-dimensional hypersurface and  $h$  is determinant of the induced metric. By CA proposal one can compute the complexity growth rate:

$$\frac{dC}{dt} = \frac{1}{\pi} \frac{dS_{\text{total}}}{dt}. \quad (18)$$

By knowing the fact that  $\frac{dr_m}{dt} = \frac{f(r_m)}{2}$ , complexity growth rate is given (for details see appendix A):

$$\begin{aligned} \frac{dS_{\text{total}}}{dt} &= \frac{V_d}{8\pi G} \sqrt{\frac{\omega^d}{\kappa}} \frac{dz + 1 - \theta - \frac{\theta}{dz}}{z r_h^{d + (\frac{1-\theta}{z})}} \left( 1 + \frac{1}{2} \left( \frac{r_h}{r_m} \right)^{\frac{dz+1-\theta}{z}} f(r_m) \left( \frac{\theta - 1 - dz + z}{dz + 1 - \theta - \frac{\theta}{dz}} \right) (\log \omega - \log f(r_m)) \right) \\ &+ \frac{6\omega z e^{\tau c_3} c_2^{\tau c_1} r_h^{\tau c_1 + \frac{2\theta}{dz}}}{\frac{d}{z} (dz + 1 - \theta - \frac{\theta}{dz}) (\tau c_1 - dz - 1 + \theta + \frac{2\theta}{d})} \left( \frac{r_h}{r_m} \right)^{\frac{dz+1-\theta}{z} - \tau c_1 - \frac{2\theta}{dz}}. \end{aligned} \quad (19)$$

In Fig.(2a) we set  $c_1 = c_3 = 1$ . As it is shown, the Lloyd bound is respected in these models for different values of parameters. Moreover, Fig.(2b) shows the violation of the Lloyd bound in the large anisotropy. The difference between small and large anisotropy effects on complexity arises due to the phase transition of confinement-deconfinement type in the system.

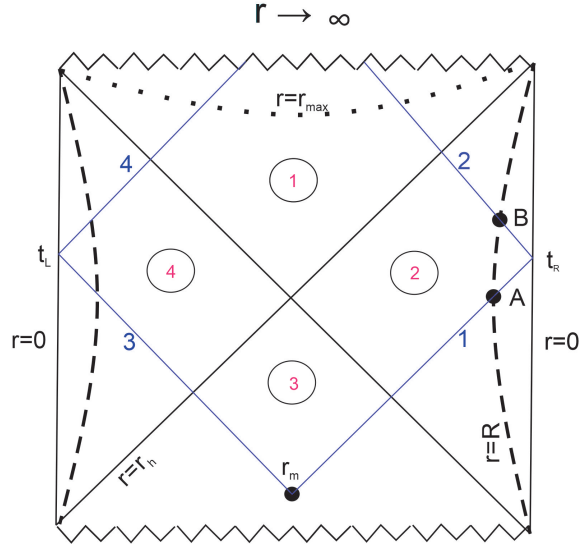


Figure 1: WDW patch of a two sided black brane.

### 3 Complexity for Vaidya metric

Vaidya metric describes formation of a black hole which implies the mass of the system increases in time. In addition, the metric could correspond a gravitational description for a global quantum quench in a field theory that means exiting a system out of equilibrium and let it evolve in time. Study of global quenches provides an understanding of how closed quantum systems reach equilibrium. Furthermore, owing to the fact that the complexity grows for a long time after equilibrium, it is expected that considering complexity growth rate for these systems does not come up with a new insight. Nonetheless, they can provide an examination of the Lloyd bound.

For the action (2) by adding an infalling null shell, the metric is given by:

$$ds^2 = \omega r^{\frac{2\theta}{d}} \left( -\frac{f}{r^2} dv^2 - \frac{2dvdr}{r^2} + \frac{d\vec{x}^2}{r^2} + \frac{dy^2}{\kappa r^{\frac{2}{d}}} \right), \quad (20)$$

in which the function  $f$  would be:

$$f(r, v) = \begin{cases} 1 & v < 0 \\ 1 - \left(\frac{r}{r_h}\right)^{d+\frac{1-\theta}{z}} & v > 0 \end{cases} \quad (21)$$

The total action in Vaidya metric would be:

$$S_{\text{total}} = S^{v>0} + S^{v<0}. \quad (22)$$

The complexity growth rate is time derivative of the complexity; moreover, by invoking relation  $\frac{dr_P}{dt} = \frac{f(r_P)}{2}$  one has (for details see appendix B):

$$\frac{dS_{\text{total}}}{dt} = \frac{V_d}{8\pi G} \sqrt{\frac{\omega}{\kappa}} \frac{\left(\frac{dz+1-\theta-\frac{\theta}{d}}{z}\right)}{r_h^{\frac{dz+1-\theta}{z}}} \left( 1 + \frac{1}{2} \left( \frac{dz-\theta+1-z}{dz-\theta+1-\frac{\theta}{d}} \right) \left( \frac{r_h}{r_P} \right)^{\frac{dz+1-\theta}{z}} f(r_P) \log f(r_P) \right). \quad (23)$$

The complexity growth rate in Vaidya solution could be seen in Fig(4).

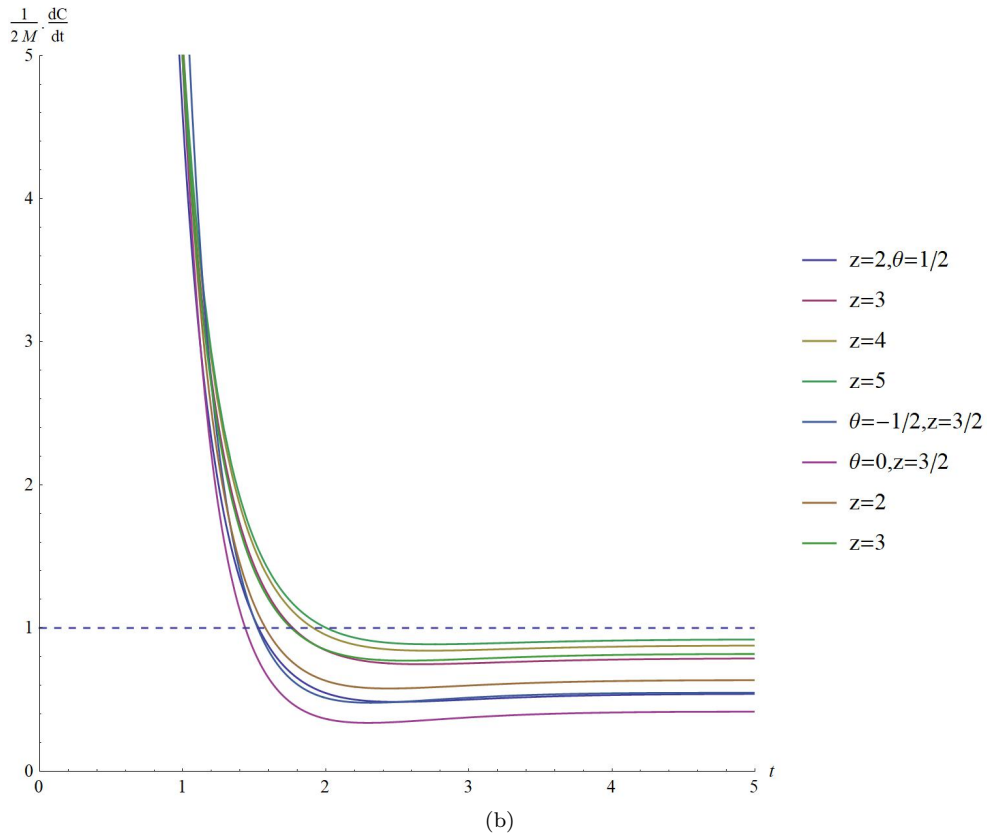
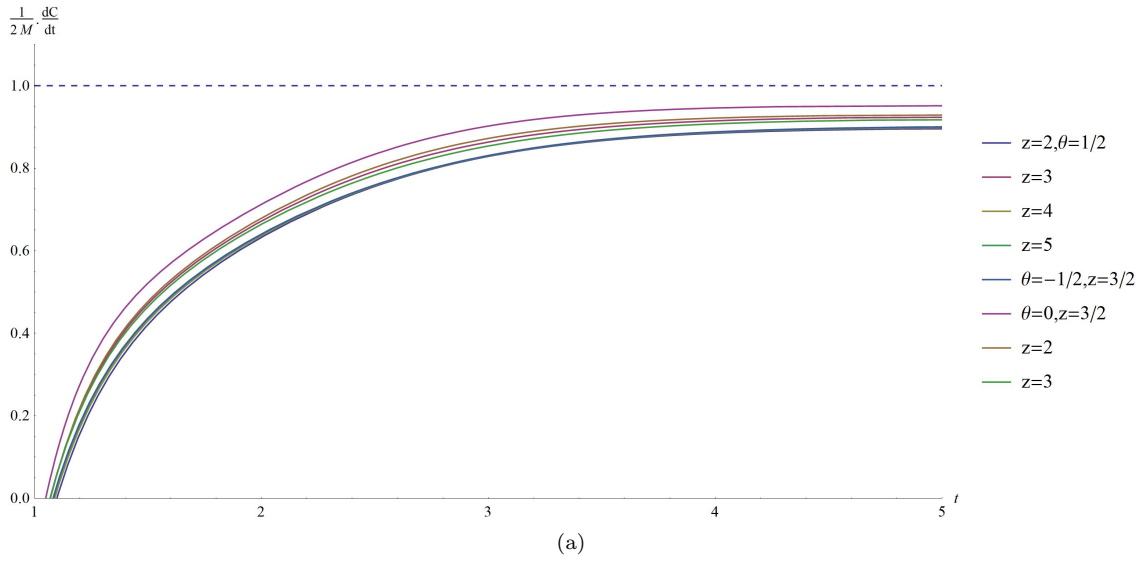


Figure 2: Complexity growth rate of the two-sided black brane for different values of  $z$  and  $\theta$  (a)  $c_2 = 1$ , (b)  $c_2 = 10$ .

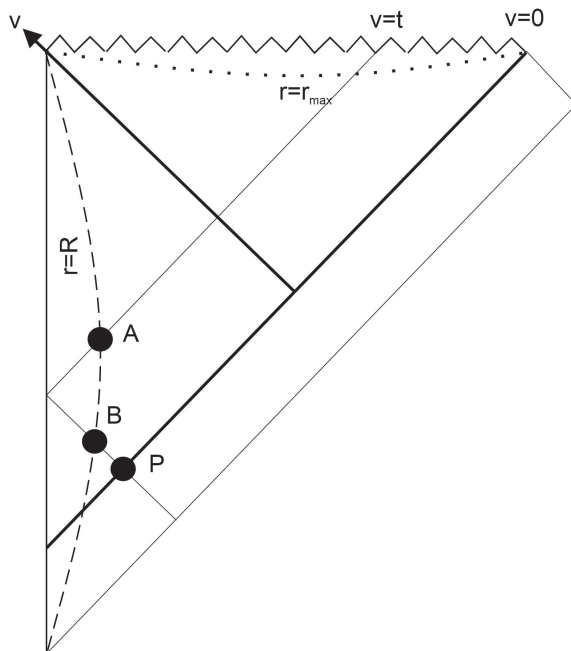


Figure 3: WDW patch of a one sided black brane.

Due to the fact that the anisotropy parameter only appears in the mass of the black brane (7) in eq. (23), then  $\frac{1}{M} \frac{dC}{dt}$  on the contrary of the two-sided black brane is independent of the anisotropy, in other words although the complexity growth rate increases with the increase in the anisotropy parameter, the Lloyd bound (complexity growth rate divided by the mass of the system) is independent of the anisotropy parameter and the Lloyd bound is satisfied. The behavior originates from the injection of energy globally in the system which is dual to the formation of the black brane. In this manner the effects of the increase in the degrees of freedom due to the mass of the black brane is dominant to the effects of the anisotropy due to the dilaton field.

## 4 Physical reasons behind the complexity and IAC

The effect of the anisotropy on the complexity growth rate for different values of  $c_2$  has been shown in Fig(5) and a turning point which could be addressed to the confinement-deconfinement phase transition as reported in [28]. Fig(5) depicts that complexity growth rate decreases when the anisotropy increases; in addition, the complexity itself decreases as anisotropy increases (see appendix A):

$$S_{\text{total}} \approx c_2^{-d+1 \frac{\theta-1}{z}} \log(c_2), \quad (24)$$

put it another way, target states get closer to the reference state in complexity space. In view of the fact that our solution is non-perturbative, then by very large anisotropy parameter, the complexity growth rate would be unity.

<sup>2</sup>By  $M$  we mean the value that the complexity growth rate saturates at late times. However, one can consider the mass of the black brane in terms of  $v$  as  $M(v) = \frac{M}{2} \left(1 + \tanh\left(\frac{v}{v_0}\right)\right)$  where  $v_0$  refers to the thickness of the infalling dust and if it goes to zero we get the step function (21). Nonetheless, the result gets some correction but the functionality to the anisotropy parameter and time would not change.

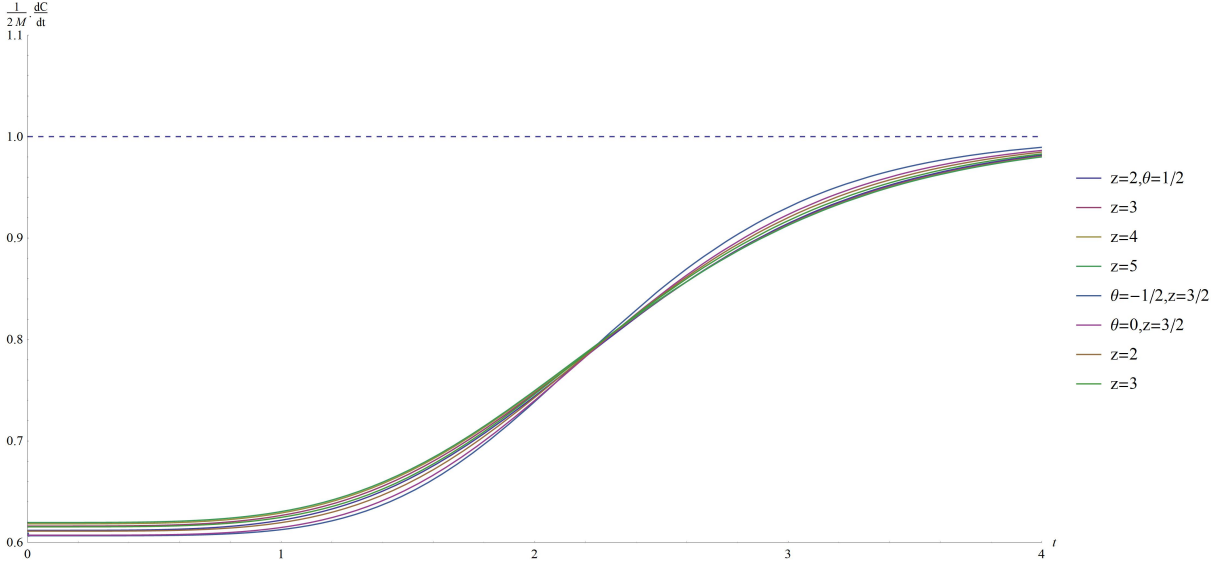


Figure 4: Complexity growth rate of Vaidya metric for different values of  $z$  and  $\theta$  in terms of the final energy of the system.

In the following the physical reasons behind the behavior of the complexity growth rate are regarded by the coupling role and considering the system degrees of freedom.

## 4.1 Coupling

The physical reason behind the overall effect is due to the dilaton field in string theory that illustrating how open strings are coupled to each other. The more value of  $c_2$  (the more coupling of open strings), the more difficulty reaching to the target state [40]. The same result about effect of dilaton on complexity has been shown in [41]. However, around  $c_2 = 1$  there is an increase in complexity growth rate. The same behavior appears in [42] where their solution is perturbative of order  $O(c_2^2)$ . This increase could be addressed to the mass of the black brane (7), in other words, away from  $c_2 = 1$  the mass of the black brane makes large contribution towards the complexity growth rate. Although in our work the solution (12) is in IR limit, that is not perturbative. Interestingly, in [42] for large anisotropy parameter their model displays a conformal anomaly and they expected that it leads to the violation of the Lloyd bound. Here, we show that the violation of the Lloyd bound for large anisotropy could be seen in Fig (2b).

The effect of coupling on the complexity could be explained by energy-time uncertainty relation in quantum mechanics. The minimum time it takes the system from an initial state goes to another state is given by:

$$\Delta t \sim \frac{\hbar}{\Delta E}. \quad (25)$$

In Zeeman (or Stark) effect energy levels of the system are corrected, for example in Hydrogen atom in weak field approximation by [43]:

$$E_n = -\frac{13.6eV}{n^2} + \mu B(m_l + 2m_s). \quad (26)$$

When the energy levels are changed the time it takes the system undergoes the time evolution is changed, then the complexity growth rate is varied<sup>3</sup>. Nonetheless, this is in no contradiction

<sup>3</sup>When the coupling is changed the Hilbert space of the system is varied, then it is convenient to see the

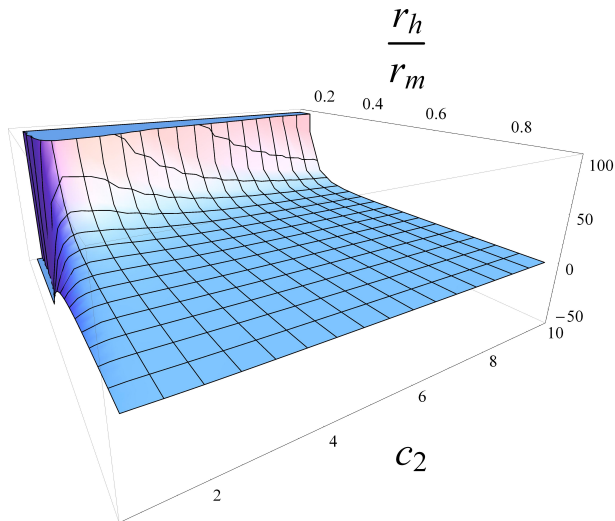


Figure 5: Complexity growth rate density ( $\frac{1}{V} \frac{dC}{dt}$ ) of two-sided black brane for values of  $z = 2$  and  $\theta = 1/2$  in terms of anisotropy parameter  $c_2$ .

with the Jackiew-Taitelboim (JT) gravity and its dual ensemble of random coupling quantum theories [45], since the holographic complexity of JT gravity is an averaging of complexity of the ensemble members [46].

Moreover, Vaidya solutions study the thermalization of systems. (23) shows that the complexity growth rate decreases as the anisotropy increases:

$$\frac{dS_{\text{total}}}{dt} \propto c_2^{-d+1 \frac{\theta-1}{z}}. \quad (27)$$

As anisotropy grows the coupling of open strings is intensified which means that the number of operators acting on states in time (complexity growth rate) decreases. It seems that as the anisotropy and the coupling increase the thermalization time decreases [49] because of the fact that the more strong coupling the more rapid thermal spreading and as a consequence the number of quantum gates (operators) required to turn the reference state to the target state decreases.

## 4.2 Degrees of freedom

One can show that the complexity growth rate at late times is proportional to the number of degrees of freedom in an Einstein-Dilaton gravity [47]:

$$\frac{1}{T^4} \frac{dC}{dt} \propto N^2, \quad (28)$$

---

complexity is about what states. Moreover, when the coupling makes changes of the complexity growth rate, the question would be: is this difference attributed to different states or gates? It means that due to the different reference and target states the complexity undergoes a change or due to the different gates. By energy-time uncertainty relation (25) we argued that the states are changed so that, say, the ground state in Hilbert space  $\mathcal{H}_{B_1}$  with coupling  $B_1$  goes to the first excited state in  $\mathcal{H}_{B_1}$  and correspondingly the ground state in Hilbert space  $\mathcal{H}_{B_2}$  with coupling  $B_2$  goes to the first excited state in  $\mathcal{H}_{B_2}$ . It is true that the two Hilbert spaces are different but there is a correspondence between the states in the unperturbed and perturbed one in quantum perturbation theory. However, in the bulk side and holographic complexity there are ambiguities in quantum gates and the reference state [6].

where  $N$  is the group rank of dual CFT and roughly speaking the number of degrees of freedom. If one takes this as an assumption then there would be:

$$\frac{dC}{dt} \propto M \propto N^2. \quad (29)$$

The above relation and Fig(5) show that as anisotropy parameter grows, the number of degrees of freedom is reduced. By thermodynamics of black holes we can see that for our black brane:

$$\frac{M}{T^4} = \frac{s}{T^3} \propto N^2. \quad (30)$$

However, this result is in glaring contradiction with Fig(5) where at large anisotropy, the complexity in the deconfinement phase is lower than the confinement phase. Nonetheless, if one omits the effect of mass of the black brane and plots  $\frac{1}{M} \frac{dC}{dt}$  in terms of the anisotropy, it makes sense<sup>4</sup>.

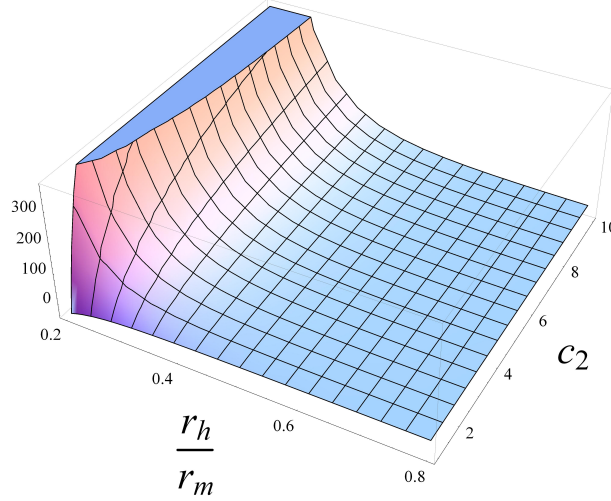


Figure 6: Complexity growth rate divided by the mass of two-sided black brane  $\frac{1}{M} \frac{1}{V} \frac{dC}{dt}$  for values of  $z = 2$  and  $\theta = 1/2$  in terms of anisotropy parameter  $c_2$ .

As in Fig(6), it is manifest that at large anisotropy where the system is in the deconfinement phase,  $\frac{1}{M} \frac{dC}{dt}$  increases. Then, it is suggested that one should interpret  $\frac{1}{M} \frac{dC}{dt}$  as the degrees of freedom.

To support this idea one can consider IAC which gives rise to the fact that by increase in anisotropy, the critical temperature decreases, then it expects that at a constant temperature, increase in the anisotropy grows the degrees of freedom. This tendency could be seen in Fig(7) that shows the behavior of  $\frac{1}{M} \frac{dC}{dt}$  in terms of anisotropy and temperature.

Whereas, the complexity growth rate decreases by the increase in the anisotropy at a constant temperature as Fig(8) shows, the degrees of freedom increases which means that the complexity growth rate itself could not be interpreted as the degrees of freedom.

Furthermore, in Vaidya solution we have seen that  $\frac{1}{M} \frac{dS_{\text{total}}}{dt}$  is independent of anisotropy then it means that the degrees of freedom in the system do not change when the anisotropy varies and unlike the two-sided black brane solution there is only one behavior of the complexity growth rate. This behavior could be addressed to the lack of phase transition in the one-sided

<sup>4</sup>It worth mentioning that the energy of the system  $M$  is constant for a fixed anisotropy parameter; however, different anisotropy parameters refer to different systems. In this manner, comparing the different systems makes  $M$  come into play.

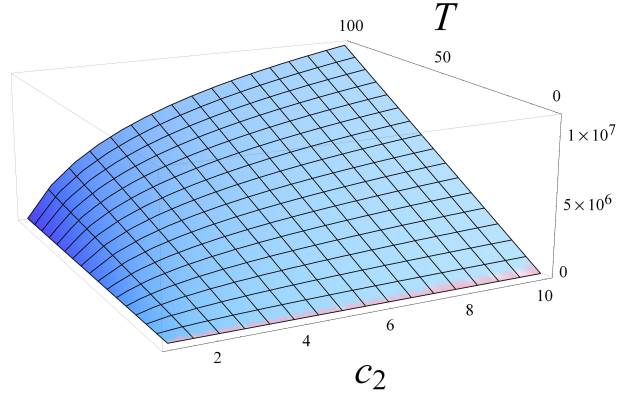


Figure 7:  $\frac{1}{M} \frac{1}{V} \frac{dC}{dt}$  in terms of anisotropy parameter  $c_2$  and temperature for values of  $z = 2$  and  $\theta = 1/2$ .

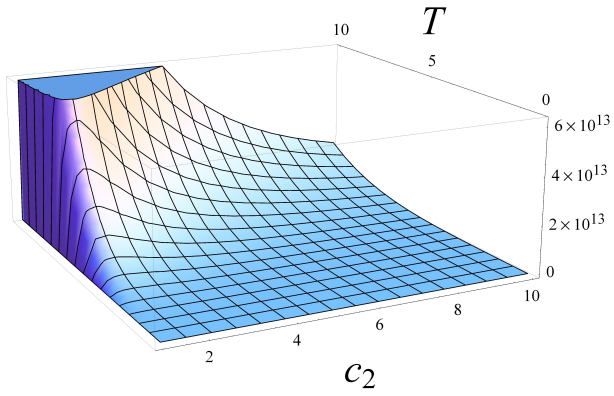


Figure 8:  $\frac{1}{V} \frac{dC}{dt}$  in terms of anisotropy parameter  $c_2$  and temperature for values of  $z = 2$  and  $\theta = 1/2$ .

solution. The formation of the black brane is dual to the injection of energy in the boundary and the system from the ground state in the boundary ((21) with condition  $v < 0$  in the bulk) goes to an excited state in the boundary with temperature  $T$  ((21) with  $v > 0$ ) where the state has different temperature and free energy, as it has been revealed in [32]<sup>5</sup>.

## 5 Conclusion

In this work we have studied anisotropic effect on complexity growth rate. The theory of Einstein-Dilaton-Axion has been considered with an Lifshitz anisotropic hyperscaling violation metric and exact dilaton solution in IR limit in term of anisotropy parameter. Because of confinement-deconfinement phases in two-sided black brane there are two different behaviors of the complexity growth rate. In small anisotropy parameters, complexity growth rate respects the Lloyd bound and in large anisotropy parameters it violates. Nonetheless, the Lloyd bound is independent of the anisotropy in the one-sided black brane which is dual to a global quantum quench on the boundary. This stems from the fact that the system does not experience a phase transition under global quantum quench by the injection of energy on the boundary.

By the way, in the extreme case when the anisotropy is large, the complexity growth rate tends to unity which means that there would not be any effort to reach the target state. In Fig(5) it could be seen that near  $c_2 = 1$  call it near isotropy, in two-sided black brane there is a direct relation, in other words, the behavior of the complexity is similar to the case of the isotropic one. Moreover, the Lloyd bound in the near isotropy, just like the isotopic one is respected. Although the same result appears in [42], their solution is perturbative in anisotropic parameter and they regarded this effect near the isotropy; however, as anisotropy grows, the contribution of the mass of the black brane dominates and the relation between anisotropy and complexity growth rate would be inversed. Actually the parameter  $c_2$  (anisotropy parameter) appears in the mass of the black brane (the coefficient of the complexity growth rate in (19)), so the increase in anisotropy shows itself in the mass of the black brane. The physical explanation of this effect is due to role of dilaton field in string theory and the number of degrees of freedom on the boundary field theory. As anisotropy parameter grows, the value of dilaton field increases and owing to the fact that dilaton field is in charge of open strings coupling, the open strings would be more coupled which means difficulty of going from reference state to the target would be more severe and as a consequence the complexity growth rate decreases. In [42] for the values of anisotropy parameter far away from isotropy, their model shows a conformal anomaly which they expect this leads to the Lloyd bound violation; however, due to the fact that they computed perturbatively they could not show that. In Fig (2b) the violation has occurred.

It has been suggested that the complexity growth rate itself is not a proper representation of system degrees of freedom but  $\frac{1}{M} \frac{dC}{dt}$ . This quantity by increase in anisotropy grows which means that according to IAC when the anisotropy parameter increases the critical temperature decreases then it is envisaged at a constant temperature when the anisotropy increases the confinement-deconfinement crossover would lead to a grow in the system degrees of freedom as depicted in Fig(7). However, in the one-sided black brane dual of a global quantum quench there is no phase transition which is due to the energy injection on the boundary. Then as a consequence, the complexity growth rate is independent of the anisotropy.

## Acknowledgment

The author would like to thank Juan Pedraza and Mostafa Ghasemi for useful discussions and Hamed Zolfi for careful reading the manuscript.

---

<sup>5</sup>[32] considers quantum phase transition through entanglement entropy; however, thermal phase transitions could be demonstrated in the phase transitions of the entanglement entropy[48].

## A Action computation for two-sided black brane

The contribution of space-like surface  $r = r_{max}$  is given:

$${}_m n_\mu = \sqrt{\frac{\omega}{f}} r^{\frac{\theta}{dz}-1} dr. \quad (\text{A-1})$$

$$K = h^{ab} K_{ab} = h^{ab} n_\mu \Gamma_{ba}^\mu = \frac{-r^{1-\frac{\theta}{dz}}}{2\sqrt{\omega f}} \left( f' - \frac{2f}{r} \left( \frac{d^2 z - d\theta + d - \theta}{dz} \right) \right), \quad (\text{A-2})$$

where  ${}_m n^\mu$  is a normal vector to  $r = r_{max}$ ,  $a, b$  are integers in  $1, \dots, d+1$  and  $\mu$  in  $1, \dots, d+2$ . Then GHY term leads to<sup>6</sup>:

$$S_{\text{GHY}} = \frac{V_d}{8\pi G} \sqrt{\frac{\omega^d}{\kappa}} \frac{1}{r^{d-1+\frac{1}{z}-\frac{\theta}{z}}} \left( f' - \frac{2f}{r} \left( \frac{d^2 z - d\theta + d - \theta}{dz} \right) \right) \left( \frac{t}{2} + r^*(R) - r^*(r) \right) \Big|_{r=r_{max}}, \quad (\text{A-3})$$

$$= \frac{V_d}{8\pi G} \sqrt{\frac{\omega^d}{\kappa}} \frac{\left( d + \frac{1}{z} - \frac{\theta}{z} - \frac{2\theta}{dz} \right)}{r_h^{d+(\frac{1-\theta}{z})}} \left( \frac{t}{2} + r^*(R) - r^*(r_{max}) \right). \quad (\text{A-4})$$

Contribution of GHY term for  $r = R$  is time-independent and because of the fact that we are interested in complexity growth rate, it is not needed to compute.

The null boundaries of WDW patch in the bottom of figure (1) are given by:

$$t_R - t = r^*(R) - r^*(r), \quad t + t_L = r^*(L) - r^*(r). \quad (\text{A-5})$$

Then normal vectors to these surfaces are:

$$n_1^\mu = A \frac{r^{2-\frac{2\theta}{dz}}}{\omega} \left( \frac{1}{f} \partial_t + \partial_r \right), \quad n_3^\mu = B \frac{r^{2-\frac{2\theta}{dz}}}{\omega} \left( \frac{1}{f} \partial_t - \partial_r \right), \quad (\text{A-6})$$

where  $A$  and  $B$  are constant. Contribution of joint points to the action are due to the points  $r_m$ ,  $A$  and  $B$ . In the following  $r_m$ 's portion is given:

$$S_{r_m} = \frac{1}{8\pi G} \int d^d x \sqrt{-\gamma} \log \left| \frac{n_1 \cdot n_3}{2} \right|, \quad (\text{A-7})$$

which leads to:

$$S_{r_m} = \frac{V_d}{8\pi G} \sqrt{\frac{\omega^d}{\kappa}} r^{\frac{\theta-1-dz+z}{z}} \left( \left( 1 - \frac{\theta}{dz} \right) \log(r^2) - \log f(r) + \log \left( \frac{AB}{\omega} \right) \right) \Big|_{r=r_m}. \quad (\text{A-8})$$

Normal vector to the surface  $r = R$  would be:

$$n_{R\mu} = \sqrt{\frac{\omega}{f}} r^{\frac{\theta}{dz}-1} dr, \quad (\text{A-9})$$

and computation of  $A$ 's portion goes as follows:

$$S_A = \frac{\text{sgn}(j)}{8\pi G} \int d^d x \sqrt{-\gamma} \log |n_1 \cdot n_R|, \quad (\text{A-10})$$

<sup>6</sup>In the following we suppose  $t_L = t_R = \frac{t}{2}$ , owing to the fact that complexity of the system is a function of  $t_L + t_R$  and for the matter of convenience we set them as  $\frac{t}{2}$ .

which is written as:

$$S_A = \frac{-V_d}{8\pi G} \sqrt{\frac{\omega^d}{\kappa}} r^{\frac{\theta-1-dz+z}{z}} \log \left( \frac{A}{\sqrt{\omega f}} r^{1-\frac{\theta}{dz}} \right) \Big|_{r=R}. \quad (\text{A-11})$$

The same calculation for joint point  $B$  occurs:

$$S_B = \frac{-V_d}{8\pi G} \sqrt{\frac{\omega^d}{\kappa}} r^{\frac{\theta-1-dz+z}{z}} \log \left( \frac{D}{\sqrt{\omega f}} r^{1-\frac{\theta}{dz}} \right) \Big|_{r=R}, \quad (\text{A-12})$$

where  $D$  is the normalization coefficient for normal vector to surface 2. The joint point contribution for points  $A$  and  $B$ <sup>7</sup> are time-independent.

To eliminate ambiguities arises by normalization of null vectors we should add some counter terms which are written as follows [38]:

$$S_{\text{null sur.}} = \frac{-1}{8\pi G} \int d\tau d^d x \sqrt{-\gamma} \Theta \log \frac{\Theta}{d-\theta}, \quad (\text{A-13})$$

where for term  $d-\theta$  we followed [12] and  $\Theta$  could be written as:

$$\Theta = \frac{1}{\sqrt{\gamma}} \frac{\partial \sqrt{\gamma}}{\partial \tau}. \quad (\text{A-14})$$

For surface 1,  $\Theta$  is given by:

$$\Theta = \frac{A}{\omega z} (\theta - 1 - dz + z) r^{1-\frac{2\theta}{dz}}, \quad (\text{A-15})$$

so the counter term for surface 1 would be:

$$S_{\text{null sur.}}^1 = \frac{V_d}{8\pi G} \sqrt{\frac{\omega^d}{\kappa}} \frac{z r^{\frac{\theta-1-dz+z}{z}}}{\theta-1-dz+z} \left( \left(1-\frac{2\theta}{dz}\right) + \left(\frac{dz+1-\theta-z}{z}\right) \log \left( \frac{A}{\omega z(d-\theta)} (\theta-1-dz+z) r^{1-\frac{2\theta}{dz}} \right) \right) \Big|_{r=R}^{r=r_m}. \quad (\text{A-16})$$

The same expression is repeated for surface 3 but the boundary would be from  $r = L$ <sup>8</sup> to  $r = r_m$ , we should note that only terms containing  $r = r_m$  are time-dependent. One can show that the similar behavior is shown up for surface 2 and 4 but by replacement of  $r_m$  for  $r_{max}$ . Furthermore, we should add some counter terms for time-like surfaces which are read as [39]:

$$S_{\text{time-like}} = -\frac{1}{16\pi G} \int d^d x dt \sqrt{-h} \left( 2d + \frac{R}{d} + O(R^2) \right), \quad (\text{A-17})$$

where  $h$  is induced metric and  $R$  is Riemann curvature of  $h$ . For surface  $r = R$ , it is read as:

$$S_{\text{time-like}} = \frac{-V_d \Delta t}{16\pi G} \sqrt{\frac{\omega^{d+1}}{\kappa}} \frac{\sqrt{f}}{r^{d+\frac{1}{z}-\frac{(d+1)\theta}{dz}}} \Big|_{r=R}, \quad (\text{A-18})$$

where  $\Delta t$  is independent of time and is given by:

$$\Delta t = 2 \int_0^{r=R} \frac{dr}{f}, \quad (\text{A-19})$$

then eq. (A-18) has no contribution to complexity growth rate. There is one step remained to have complexity growth rate and that is computing eq. (14) in WDW patch. There are four

<sup>7</sup>For their counterparts on the left side of figure (1) are time-independent too.

<sup>8</sup>It is supposed that the value of  $r = R$  and  $r = L$  are the same.

regions that their contributions would be as follows:

$$S_{\text{bulk}}^1 = -\frac{6V_d}{4\pi Gd} \sqrt{\frac{\omega^{d+2}}{\kappa}} e^{\tau c_3} c_2^{\tau c_1} \int_{r_h}^{r_{\text{max}}} r^{\frac{(d+2)\theta}{dz} - \frac{1}{z} - (d+1) + \tau c_1} \left( \frac{t}{2} + r^*(0) - r^*(r) \right) dr, \quad (\text{A-20})$$

$$S_{\text{bulk}}^2 = S_{\text{bulk}}^4 = -\frac{6V_d}{4\pi Gd} \sqrt{\frac{\omega^{d+2}}{\kappa}} e^{\tau c_3} c_2^{\tau c_1} \int_{r=R}^{r_h} r^{\frac{(d+2)\theta}{dz} - \frac{1}{z} - (d+1) + \tau c_1} \left( r^*(0) - r^*(r) \right) dr, \quad (\text{A-21})$$

$$S_{\text{bulk}}^3 = -\frac{6V_d}{4\pi Gd} \sqrt{\frac{\omega^{d+2}}{\kappa}} e^{\tau c_3} c_2^{\tau c_1} \int_{r_h}^{r_m} r^{\frac{(d+2)\theta}{dz} - \frac{1}{z} - (d+1) + \tau c_1} \left( -\frac{t}{2} + r^*(0) - r^*(r) \right) dr. \quad (\text{A-22})$$

The contribution of the whole bulk could be written in terms of time-dependent and independent terms:

$$\begin{aligned} S_{\text{bulk}} &= -\frac{6V_d}{4\pi Gd} \sqrt{\frac{\omega^{d+2}}{\kappa}} e^{\tau c_3} c_2^{\tau c_1} \int_{r_m}^{r_{\text{max}}} r^{\frac{(d+2)\theta}{dz} - \frac{1}{z} - (d+1) + \tau c_1} \left( \frac{t}{2} - r^*(0) + r^*(r) \right) dr \\ &\quad - \frac{3V_d}{\pi Gd} \sqrt{\frac{\omega^{d+2}}{\kappa}} e^{\tau c_3} c_2^{\tau c_1} \int_{r=R}^{r_{\text{max}}} r^{\frac{(d+2)\theta}{dz} - \frac{1}{z} - (d+1) + \tau c_1} \left( r^*(0) - r^*(r) \right) dr. \end{aligned} \quad (\text{A-23})$$

It is still needed to add a counter term to engender the action finite which could be written as [12]:

$$S_{\text{count.}} = \frac{1}{8\pi G} \int d\tau d^d x \sqrt{\gamma} \Theta \left( \frac{1}{2} \alpha \phi + L \right), \quad (\text{A-24})$$

which for light-like surface 1 leads to:

$$S_{\text{count.}} = -\frac{V_d}{8\pi G} \sqrt{\frac{\omega^d}{\kappa}} r^{\frac{\theta - dz - 1 + z}{z}} \left( \frac{\alpha c_1}{2} \left( \frac{z}{z + \theta - 1 - dz} + \log(c_2 r) \right) + \frac{\alpha c_3}{2} + L \right) \Big|_{r=R}^{r=r_m}. \quad (\text{A-25})$$

The coefficients  $\alpha$  and  $L$  are read as:

$$\alpha c_1 = \frac{2\theta}{dz}, \quad (\text{A-26})$$

$$2L = \log(\omega f(R)) - \frac{2z(1 - \frac{2\theta}{dz})}{dz + 1 - z - \theta} + \frac{2\theta}{d(z + \theta - 1 - dz)} - \alpha c_3 + 2 \log\left(\frac{\theta - 1 - dz + z}{\omega z(d - \theta)}\right) + \frac{2\theta}{dz} \log c_2. \quad (\text{A-27})$$

Now we are able to compute the rate of complexity by total action from eq.s (A-4) (A-8) (A-11) (A-12) (A-16) (A-18) (A-23) (A-25):

$$\begin{aligned} S_{\text{total}} &= S_{\text{GHY}} + S_{r_m} + S_A + S_B + S_{\text{null sur.}}^1 + S_{\text{null sur.}}^2 + S_{\text{null sur.}}^3 + S_{\text{null sur.}}^4 \\ &\quad + S_{\text{time-like}} + S_{\text{bulk}} + S_{\text{count.}}. \end{aligned} \quad (\text{A-28})$$

The leading term of the complexity in large anisotropy arises by counter terms (A-25):

$$S_{\text{total}} \propto \sqrt{\frac{\omega^d}{\kappa}} \log(c_2) = c_2^{-d+1 \frac{\theta-1}{z}} \log(c_2), \quad (\text{A-29})$$

which is decreasing by growing the anisotropy.

## B One-sided black brane

It is needed to consider the patches  $v > 0$  and  $v < 0$ .

$v > 0$

For  $v > 0$  there are five boundaries:  $v = 0$ ,  $v = t$ ,  $r = R$ ,  $r = r_m$  and line going through  $BP$  which is given by:

$$t - v = 2 \int_R^{r(v)} \frac{dr}{f}. \quad (\text{B-30})$$

Normal vector to surface  $r = r_{max}$  would be:

$$n_m^\mu = \frac{r^{1-\frac{\theta}{dz}}}{\sqrt{\omega}} \left( -\frac{1}{\sqrt{f}} \partial_v + \sqrt{f} \partial_r \right), \quad (\text{B-31})$$

and extrinsic curvature reads as:

$$K = h^{ab} K_{ab} = -\sqrt{\frac{\omega}{f}} \frac{r^{1-\frac{\theta}{dz}}}{2\omega} \left( f' - \frac{2f}{r} \left( \frac{d^2 z - d\theta + d - \theta}{dz} \right) \right). \quad (\text{B-32})$$

Put these all in eq. (A-4):

$$\begin{aligned} S_{\text{GHY}} &= \frac{V_d}{16\pi G} \sqrt{\frac{\omega^d}{\kappa}} r^{\frac{\theta-1}{z}+1-d} \left( f' - \frac{2f}{r} \left( \frac{d^2 z - d\theta + d - \theta}{dz} \right) \right) t \Big|_{r=r_{max}} \\ &= \frac{V_d}{16\pi G} \sqrt{\frac{\omega^d}{\kappa}} \frac{t}{r_h^{d+\frac{1-\theta}{z}}} \left( \frac{dz - \theta + 1 - \frac{2\theta}{d}}{z} \right). \end{aligned} \quad (\text{B-33})$$

For joint points, normal vector to the surfaces is needed. Normal vectors to  $v = 0$  ( $v = t$ ),  $BP$  and  $r = R$  respectively are given:

$$n_0^\mu = -\frac{B r^{2-\frac{2\theta}{dz}}}{\omega} \partial_r \quad (\text{B-34})$$

$$n_{BP}^\mu = \frac{C r^{2-\frac{2\theta}{dz}}}{\omega} \left( -\frac{2}{f} \partial_v + \partial_r \right) \quad (\text{B-35})$$

$$n_R^\mu = \frac{r^{1-\frac{\theta}{dz}}}{\sqrt{\omega}} \left( -\frac{1}{\sqrt{f}} \partial_v + \sqrt{f} \partial_r \right). \quad (\text{B-36})$$

Then, the contribution of joint points for point  $P$  would be:

$$S_P^{v>0} = \frac{V_d}{8\pi G} \sqrt{\frac{\omega^d}{\kappa}} r^{\frac{\theta-1}{z}+1-d} \left( \left(1 - \frac{\theta}{dz}\right) \log r^2 - \log f(r) + \log \frac{BC}{\omega} \right) \Big|_{r=r_P}. \quad (\text{B-37})$$

The contribution of points  $A$  and  $B$  would be similar which is given by:

$$S_A = \frac{V_d}{8\pi G} \sqrt{\frac{\omega^d}{\kappa}} r^{\frac{\theta-1}{z}+1-d} \left( \left(1 - \frac{\theta}{dz}\right) \log r - \log \sqrt{f(r)} + \log \frac{B}{\sqrt{\omega}} \right) \Big|_{r=R}, \quad (\text{B-38})$$

which is time-independent, then the joint point contribution for point  $A$  and  $B$  are negligible for complexity growth rate. The bulk action contribution to complexity as shown in eq. (14) goes as follows:

$$S_{\text{bulk}} = -\frac{3V_d}{4\pi G d} \sqrt{\frac{\omega^{d+2}}{\kappa}} e^{\tau c_3} c_2^{\tau c_1} \int dv \int dr r^{\frac{(d+2)\theta}{dz} - \frac{1}{z} - d - 1 + \tau c_1}. \quad (\text{B-39})$$

For region  $v > 0$ , it leads to:

$$S_{\text{bulk}}^{v>0} = -\frac{3V_d}{4\pi Gd} \sqrt{\frac{\omega^{d+2}}{\kappa}} e^{\tau c_3} c_2^{\tau c_1} \left\{ \int_0^{v_B} dv \int_{r(v)}^\infty dr r^{\frac{(d+2)\theta}{dz} - \frac{1}{z} - d - 1 + \tau c_1} \right. \\ \left. + \int_{v_B}^t dv \int_{r_B=R}^\infty dr r^{\frac{(d+2)\theta}{dz} - \frac{1}{z} - d - 1 + \tau c_1} \right\}, \quad (\text{B-40})$$

where  $v_B \approx t - 2r_B$ . By assumption  $\frac{(d+2)\theta}{dz} - \frac{1}{z} - d - 1 + \tau c_1 < -1$ , one can get to the following result:

$$S_{\text{bulk}}^{v>0} = \frac{3V_d}{4\pi Gd} \sqrt{\frac{\omega^{d+2}}{\kappa}} \frac{e^{\tau c_3} c_2^{\tau c_1}}{\left(\frac{(d+2)\theta}{dz} - \frac{1}{z} - d + \tau c_1\right)} \left\{ \int_0^{v_B=t-2r_B} dv r(v)^{\frac{(d+2)\theta}{dz} - \frac{1}{z} - d + \tau c_1} + 2r_B^{\frac{(d+2)\theta}{dz} - \frac{1}{z} - d + 1 + \tau c_1} \right\} \\ = \frac{6V_d}{4\pi Gd} \sqrt{\frac{\omega^{d+2}}{\kappa}} \frac{e^{\tau c_3} c_2^{\tau c_1}}{\left(\frac{(d+2)\theta}{dz} - \frac{1}{z} - d + \tau c_1\right)} \left\{ \frac{r_P^{\frac{(d+2)\theta}{dz} - \frac{1}{z} - d + 1 + \tau c_1}}{\left(\frac{(d+2)\theta}{dz} - \frac{1}{z} - d + 1 + \tau c_1\right)} + r_B^{\frac{(d+2)\theta}{dz} - \frac{1}{z} - d + 1 + \tau c_1} \right\}. \quad (\text{B-41})$$

$v < 0$

In this region the function  $f$  is 1 and the work is easier. The contribution of joint point  $P$  is similar to its counterpart in  $v > 0$  but for  $f = 1$  and a minus, so it is written as:

$$S_P^{v<0} = \frac{-V_d}{8\pi G} \sqrt{\frac{\omega^d}{\kappa}} r^{\frac{\theta-1}{z} + 1 - d} \left( \left(1 - \frac{\theta}{dz}\right) \log r^2 + \log \frac{BC}{\omega} \right) \Big|_{r=r_P}. \quad (\text{B-42})$$

Finally, one can compute the bulk contribution of complexity in the region  $v < 0$ :

$$S_{\text{bulk}}^{v<0} = -\frac{3V_d}{4\pi Gd} \sqrt{\frac{\omega^{d+2}}{\kappa}} e^{\tau c_3} c_2^{\tau c_1} \int_{-\infty}^0 dv \int_{r_P - \frac{v}{2}}^\infty r^{\frac{(d+2)\theta}{dz} - \frac{1}{z} - d - 1 + \tau c_1} \\ = \frac{-6V_d}{4\pi Gd} \sqrt{\frac{\omega^{d+2}}{\kappa}} e^{\tau c_3} c_2^{\tau c_1} \frac{r_P^{\frac{(d+2)\theta}{dz} - \frac{1}{z} - d + 1 + \tau c_1}}{\left(\frac{(d+2)\theta}{dz} - \frac{1}{z} - d + \tau c_1\right) \left(\frac{(d+2)\theta}{dz} - \frac{1}{z} - d + 1 + \tau c_1\right)}. \quad (\text{B-43})$$

## References

- [1] J. M. Maldacena, "The Large N Limit of Superconformal Field Theories and Supergravity," Adv.Theor.Math.Phys.2:231-252,1998, arXiv:9711200v3[hep-th].
- [2] L. Susskind, "Three Lectures on Complexity and Black Holes," arXiv:1810.11563[hep-th].
- [3] L. Susskind and D. Stanford, "Complexity and shock wave geometry," Phys. Rev. D 90, 126007 (2014), arXiv:1406.2678[hep-th].
- [4] A. R. Brown, D. A. Roberts, L. Susskind, B. Swingle, and Y. Zhao, "Complexity Equals Action," Phys. Rev. Lett. 116, 191301 (2016), arXiv:1509.07876 [hep-th].
- [5] J. C., W. Fischler and P. H. Nguyen, "Noether charge, black hole volume, and complexity," JHEP 1703 (2017) 119, arXiv:1610.02038[hep-th].
- [6] A. Belin, R. C. Myers, S.-M. Ruan, G. Sárosi, and A. J. Speranza, "Does Complexity Equal Anything?," Phys.Rev.Lett. 128 (2022) 8, 081602, arXiv: 2111.02429 [hep-th]
- [7] S. Lloyd, "Ultimate physical limits to computation," Nature 406 (Aug., 2000), arXiv:9908043[quant-ph].

- [8] D. Carmi, S. Chapman, H. Marrochio, R. C. Myers, and S. Sugishita, "On the Time Dependence of Holographic Complexity," JHEP 1711 (2017) 188, arXiv:1709.10184 [hep-th].
- [9] M. Moosa, "Divergences in the rate of complexitication," Phys. Rev. D 97, 106016 (2018), arXiv:1712.07137[hep-th].
- [10] M. Ghodrati, "Complexity growth in massive gravity theories, the effects of chirality, and more," Phys. Rev. D 96, no. 10, 106020 (2017).
- [11] R. Q. Yang, C. Niu, C. Y. Zhang, and K. Y. Kim, "Comparison of holographic and field theoretic complexities for time-dependent thermofield double states," JHEP 1802, 082 (2018).
- [12] M. Alishahiha, A. Faraji Astaneh, M. R. Mohammadi Mozaffar, and A. Mollabashi, "Complexity Growth with Lifshitz Scaling and Hyperscaling Violation," JHEP 1807 (2018).
- [13] R.-Q. Yang, C. Niu, C.-Y. Zhang and K.-Y. Kim, "Comparison of holographic and field theoretic complexities by time dependent thermofield double states," JHEP 02 (2018) 082, arXiv:1710.00600v2 [hep-th].
- [14] A. Akhavan, M. Alishahiha, A. Naseh and H. Zolfi, "Complexity and behind the horizon cut off", JHEP12(2018)090.
- [15] J. Couch, S. Eccles, T. Jacobson and P. Nguyen, "Holographic Complexity and Volume," JHEP 11 (2018) 044, arXiv:1807.02186v2 [hep-th].
- [16] A. Karch and A. O'Bannon, "Metallic AdS/CFT," JHEP 09 (2007) 024 [0705.3870].
- [17] T. Albash, V. G. Filev, C. V. Johnson, and A. Kundu, "Quarks in an external electric field in finite temperature large N gauge theory," JHEP 08 (2008) 092 [0709.1554].
- [18] E. D'Hoker and P. Kraus, "Magnetic Brane Solutions in AdS," JHEP 10 (2009) 088, arXiv:0908.3875[hep-th].
- [19] K. Jensen, A. Karch, and E. G. Thompson, "A Holographic Quantum Critical Point at Finite Magnetic Field and Finite Density," JHEP 05 (2010) 015, arXiv:1002.2447[hep-th].
- [20] K.-Y. Kim, B. Sahoo, and H.-U. Yee, "Holographic chiral magnetic spiral," JHEP 10 (2010) 005, arXiv:1007.1985[hep-th].
- [21] N. Evans, K.-Y. Kim, J. P. Shock, and J. P. Shock, "Chiral phase transitions and quantum critical points of the D3/D7(D5) system with mutually perpendicular E and B fields at finite temperature and density," JHEP 09 (2011) 021, arXiv:1107.5053[hep-th].
- [22] A. Donos, J. P. Gauntlett, and C. Pantelidou, "Magnetic and Electric AdS Solutions in String- and M-Theory," Class. Quant. Grav. 29 (2012) 194006, arXiv:1112.4195[hep-th].
- [23] U. Gursoy, M. Jarvinen, G. Nijs, and J. F. Pedraza, "Inverse Anisotropic Catalysis in Holographic QCD," JHEP 04 (2019) 071, arXiv:1811.11724v3.
- [24] D. Mateos and D. Trancanelli, "Thermodynamics and Instabilities of a Strongly Coupled Anisotropic Plasma," JHEP 07 (2011) 054, arXiv:1106.1637[hep-th].
- [25] P. Liu, C. Niu, and J.-P. Wu, "The Effect of Anisotropy on Holographic Entanglement Entropy and Mutual Information," Phys. Lett. B796 (2019) 155, arXiv:1905.06808[hep-th].
- [26] D. Roychowdhury, "Holography for anisotropic branes with hyperscaling violation," JHEP 01 (2016) 105.

- [27] A. Donos, J. P. Gauntlett, and O. Sosa-Rodriguez, "Anisotropic plasmas from axion and dilaton deformations," JHEP 11 (2016) 002.
- [28] D. Giataganas, U. Grsoy, and J. F. Pedraza, "Strongly-coupled anisotropic gauge theories and holography," Phys. Rev. Lett. 121, no. 12, 121601 (2018), arXiv:1708.05691.
- [29] D. M. Rodrigues, E. F. Capossoli, and H. Boschi-Filho, "Magnetic catalysis and inverse magnetic catalysis in (2+1)-dimensional gauge theories from holographic models," Phys. Rev. D 97, 126001.
- [30] U. Gürsoy, M. Järvinen, G. Nijs, and J. F. Pedraza, "On the interplay between magnetic field and anisotropy in holographic QCD," JHEP 2103 (2021) 180, arXiv:2011.09474v3 [hep-th].
- [31] M. J. Vasli, M. R. Mohammadi Mozaffar, K. Babaei Velni and M. Sahraei, "Holographic Study of Reflected Entropy in Anisotropic Theories," Phys.Rev.D 107 (2023) 2, 026012, arXiv:2207.14169 [hep-th].
- [32] P.-C. Sun, D.-S. Lee and C.-P. Yeh, "Holographic approach to thermalization in general anisotropic theories," JHEP 03 (2021) 164, arXiv:2011.02716v2 [hep-th].
- [33] M. Ghasemi and S. Parvizi, "Constraints on anisotropic RG flows from holographic entanglement entropy," Phys.Rev.D 104 (2021) 086028, arXiv:1907.01546v3 [hep-th].
- [34] M. Ghasemi and S. Parvizi, "Curved Corner Contribution to the Entanglement Entropy in an Anisotropic Spacetime," arXiv:1905.01675v4 [hep-th].
- [35] D. Mateos and D. Trancanelli, "Thermodynamics and Instabilities of a Strongly Coupled Anisotropic Plasma," JHEP 1107, 054 (2011), arXiv:1106.1637 [hep-th].
- [36] K. Parattu, S. Chakraborty, B. R. Majhi, and T. Padmanabhan, "A Boundary Term for the Gravitational Action with Null Boundaries," Gen. Rel. Grav. 48, no. 7, 94 (2016), arXiv:1501.01053.
- [37] L. Lehner, R. C. Myers, E. Poisson, and R. D. Sorkin, "Gravitational action with null boundaries," Phys. Rev. D 94 (2016) no.8, 084046, arXiv:1609.00207.
- [38] L. Lehner, R. C. Myers, E. Poisson, and R. D. Sorkin, "Gravitational action with null boundaries," Phys. Rev. D 94 (2016) no.8, 084046, arXiv:1609.00207 [hep-th].
- [39] M. Henningson and K. Skenderis, "The Holographic Weyl anomaly," JHEP 9807, 023 (1998), arXiv:9806087.
- [40] M. Ghodrati, "Complexity growth rate during phase transitions," PHYSICAL REVIEW D 98, 106011 (2018).
- [41] Y.-S. An and R.-H. Peng, "The effect of dilaton on the holographic complexity growth," Phys. Rev. D 97, 066022 (2018).
- [42] S. A. Hosseini Mansoori, V. Jahnke, M. M. Qaemmaqami, and Y. D. Olivas, "Holographic complexity of anisotropic black branes," Phys. Rev. D 100, 046014 (2019), arXiv:1808.00067v3.
- [43] D. J. Griffiths, "Introduction to Quantum Mechanics (2nd Edition)," Pearson Prentice Hall, 2004.
- [44] M. Moosa, "Evolution of Complexity Following a Global Quench," arXiv:1711.02668v3 [hep-th].

- [45] P. Saad, S. H. Shenker, and D. Stanford, "JT gravity as a matrix integral," arXiv:1903.11115 [hep-th].
- [46] Vijay Balasubramanian, Matthew DeCrossa, Arjun Kara and Onkar Parrikar, "Quantum Complexity of Time Evolution with Chaotic Hamiltonians," JHEP 01 (2020) 134 ,arXiv:1905.05765v3 [hep-th]
- [47] S.-J. Zhang, "Complexity and phase transitions in a holographic QCD model," Nucl.Phys. B929 (2018) 243-253, arXiv:1712.07583 [hep-th].
- [48] N. Jokela, H. Ruotsalainen and J. G. Subils "Limitations of entanglement entropy in detecting thermal phase transitions," arXiv:2310.11205v2 [hep-th].
- [49] I. Y. Aref'eva, "QGP time formation in holographic shock waves model of heavy ion collisions," Theor.Math.Phys. 184 (2015), 1239-1255, arXiv:1503.02185v1 [hep-th].